IJMTST | Volume: 2 | Issue: 07 | July 2016 | ISSN: 2455-3778

Adaptive Control Scheme for PV Based Induction Machine

M. Siva Kumar[1] | D. Ramesh[2]

[1]PG Scholar, Department of Electrical & Electronics Engineering, Malla Reddy Engineering College, Maisammaguda, Medchal (M), Rangareddy (Dt), Telangana, India.
[2]AssistantProfessor, Department of Electrical & Electronics Engineering, Malla Reddy Engineering College, Maisammaguda, Medchal (M), Rangareddy (Dt), Telangana, India.

ABSTRACT

An adaptive control scheme for maximum power point tracking of a single-phase grid-connected photovoltaic system is presented. The difficulty on design a controller that may operate a photovoltaic system on its maximum power point (MPP) is that, this MPP depends on temperature and solar irradiance, ambient conditions that are time-varying and difficult to measure. A solution using an on-line sliding mode estimator is presented. It estimates three different parameters that depend on solar irradiance and temperature, eliminating the necessity of having any sensor for these environmental variables. It is capable of estimate time-varying parameters. A complete analysis was done taking into account the non-linearity's showed by the closed-loop system. An adaptive law was found to substitute a perturbation bound and also to eliminate possible chattering due to the discontinuous controller term. Computer simulations are presented to show the good performance of the controller. The controller detects the deviation of the actual trajectory from the reference trajectory and corresponding changes the switching strategy to restore the tracking. Prominent characteristics such as invariance, robustness, order reduction, and control chattering are discussed in detail. Methods for coping with chattering are presented. Both linear and nonlinear systems are considered The proposed concept can be implemented to adaptive control scheme for induction machine using Matlab/Simulink software.

KEYWORDS: *Grid-connected photovoltaic (PV) system, matching conditions, nonlinear controller, partial feedback linearzing scheme, structured uncertainty.*

I. INTRODUCTION

The utilization of grid-connected photovoltaic (PV) systems is increasingly being pursued as a supplement and an alternative to the conventional fossil fuel generation in order to meet increasing energy demands and to limit the pollution of the environment caused by fuel emissions. The major concerns of integrating PV into the grid are stochastic behaviors of solar irradiations and interfacing of inverters with the grid. Because of the high initial investment, variations in solar irradiation, and reduced life-time of PV systems, as compared with the traditional energy sources, it is essential to extract maximum power from PV systems [1].

Maximum power point tracking (MPPT) techniques are widely used to extract maximum power from the PV system that is delivered to the grid through the inverter [2]–[4]. Recent improvements on MPPT can be seen in [5] and [6]. Interconnections among PV modules within a shaded PV field can affect the extraction of maximum power [7]. A study of all possible shading scenarios and interconnection schemes for a given PV field, to maximize the output power of PV array, is proposed in [7]. Inverters interfacing PV modules with the grid perform two major tasks—one is to ensure that PV modules are operated at maximum power point (MPP), and the other is to inject a sinusoidal current into the grid. In order to perform these tasks effectively, efficient stabilization or control schemes are essential. In a grid-connected

PV system, control objectives are met by a strategy using a pulse width modulation (PWM) scheme based on two cascaded control loops [8].

The two cascaded control loops consist of an outer voltage control loop to settle the PV array at the MPP, and an inner current control loop to establish the duty ratio for the generation of a sinusoidal output current, which is in phase with the grid voltage [8]. The current loop is also responsible for power quality issues and current protection for which harmonic compensations and dynamics are the important properties of the current controller.

Linear controllers such as proportional-integral (PI), hysteresis, and model predictive controllers are presented in [9]–[14], which provide satisfactory operation over a fixed set of operating points as the system is linearized at an equilibrium point. Since the PV source exhibits a strongly nonlinear electrical behavior due to the variation of solar irradiance and nonlinear switching functions of inverters. As linear controllers for nonlinear PV systems affects all the variables in the system and the electrical characteristics of the PV source are time varying, the system is not linearizable around a unique operating point or trajectory to achieve a good performance over a wide variation in atmospheric conditions. The restrictions of operating points can be solved by implementing nonlinear controllers for nonlinear PV systems.

A sliding-mode current controller for a grid-connected PV system is proposed in [15], along with a new MPPT technique to provide robust tracking performances. In [15], the controller is designed based on a time-varying sliding surface. However, the selection of a time-varying surface is a difficult task, and the system stays confined to the sliding surface. Feedback linearization has been increasingly used for nonlinear controller design. It transforms the nonlinear system into a fully or partly linear equivalent by canceling nonlinearities. A feedback linearizing technique was first proposed in [16] for PV applications where a superfluous complex model of the inverter is considered to design the controller. To overcome the complexity, a simple and consistent inverter model is used in [17], and a feedback linearization technique is employed to operate the PV system at MPP. In [16] and [17], a feedback linearizing controller is designed by considering the dc-link voltage and quadrature-axis grid current as output functions. Power-balance relationships are considered to express the dynamics of the voltage across the dc-link capacitor. However, this relationship cannot capture nonlinear switching functions between inverter input and output; to accurately represent a grid-connected PV system but it is essential to consider these switching actions. The current relationship between the input and output of the inverter can be written in terms of switching functions rather than the power balance equation. Therefore, the voltage dynamics of the dc-link capacitor include nonlinearities due to the switching actions of the inverter.

The inclusion of these nonlinearities in the model will improve the accuracy; however, the grid-connected PV system will be partially, rather than exactly, linearized, as presented in [18]. Although the approaches presented in [16]–[18] ensure MPP operation of the PV system, they do not account for inherent uncertainties in the system. In the design of both linear and nonlinear controllers for grid-connected PV systems, most of the difficulties stem from the analytical complexity of the dynamic model of a PV system, which, on one hand, exhibits a nonlinear parametric dependence on the PV array current–voltage characteristics varying with the irradiation and temperature levels and, on the other, a sinusoidal time dependence due to the grid connection of PV systems. These difficulties may lead to some barriers in developing a meaningful and realistic mathematical model. The mismatch between the mathematical model and true system may lead to serious stability problems for the system. Therefore, the designs of robust control strategies that consider the model uncertainties are of great importance to design nonlinear controllers. Variable structure control with sliding mode, or sliding-mode control is one of the effective nonlinear robust control approaches since it provides system dynamics with an invariance property to uncertainties once the system dynamics are controlled in the sliding mode.

A sliding-mode controller for grid connected PV system is presented in [19] and [20] to achieve robust MPPT under uncertainties within the system model. With this control approach, the insensitivity of the controlled system to uncertainties exists in the sliding mode but not during the reaching phase, i.e., the system dynamic in the reaching phase is still influenced by uncertainties. A mini-max LQG technique is proposed in [21] to design a robust controller for the integration of PV generation into the grid where the higher order terms during the linearization is considered as the uncertainty. A feed forward mechanism is proposed in [22] to control the

current and dc-link voltage and the robustness of this mechanism is analyzed through modal analysis. A robust fuzzy controlled PV inverter is presented in [23] for the stabilization of a grid connected PV system where the robustness is adopted by using the Taguchi-tuning algorithm. However, the main difficulties of the robustness algorithm, as presented in [21] [23], are the consideration of linearized PV system models that are unable to maintain the stability of the PV system over a wide changes in atmospheric conditions. Although there are some advances in the robust control of grid-connected PV systems, research into the robustness

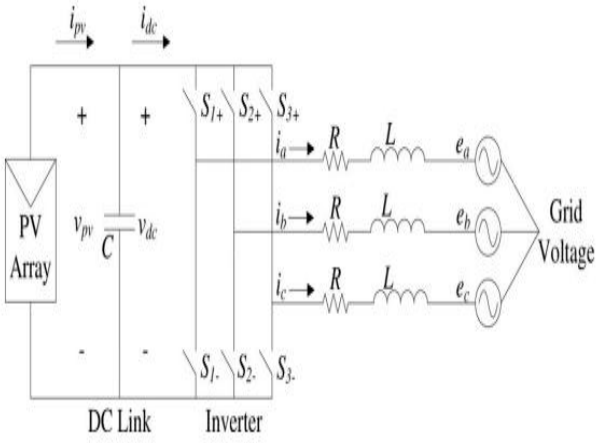

Fig. 1. Three-phase grid-connected PV system.

analysis and the controller design of nonlinear uncertain PV systems remains an important and challenging area. Since the feedback linearization technique is widely used in the design of nonlinear controllers for power systems, this paper proposed the extension of the partial feedback linearizing scheme, as presented in [18], by considering uncertainties within the PV system model. In this paper, matching conditions are used to model the uncertainties in PV systems for given upper bounds on the modeling error, which include parametric and state-dependent uncertainties. These uncertainties are bounded in such a way that the proposed controller can guarantee the stability and enhance the performance for all possible perturbations within the given upper bounds of the modeling errors of nonlinear PV systems. The effectiveness of the proposed controller is tested and compared with that of a partial feedback linearizing controller without uncertainties, following changes in atmospheric conditions.

II. Photovoltaic System Model

The schematic diagram of a three-phase grid-connected PV system, which is the main focus of this paper, is shown in Fig. 1. The considered PV system consists of a PV array, a dc-link capacitor *C*, a three-phase inverter, a filter inductor *L*, and grid voltages *ea*, *eb*, *ec*. In this paper, the main aim is to control the voltage *υ*dc (which is also the output voltage of PV array *υ*pv) across the capacitor *C* and to make the input current in phase with grid voltage for unity power factor by means of appropriate control signals through the switches of the inverter.

***A. Photovoltaic Cell and Array Model*:** A PV cell is a simple p-n junction diode that converts the irradiation into electricity. Fig. 2 shows an equivalent circuit diagram of a PV cell that consists of a light generated current source *IL*, a parallel diode, a shunt resistance *R*sh, and a series resistance *Rs*. In Fig. 2, *I*ON is the diode current that can be written as

$$I_{ON} = I_s\left[\exp\left[\alpha\left(v_{pv} + R_s i_{pv}\right)\right] - 1\right] \quad (1)$$

where $a = qAkTC$, $k = 1.3807 \times 10{-}23$ JK−1 is the Boltzmann's constant, $q = 1.6022 \times 10{-}19$ C is the charge of electron, *TC* is the cell's absolute working temperature in Kelvin, *A* is the p-n junction ideality factor whose value is between 1 and 5, *Is* is the saturation current, and *υ*pv is the output voltage of the PV array which is also the voltage across *C*, i.e., *υ*dc. Now,

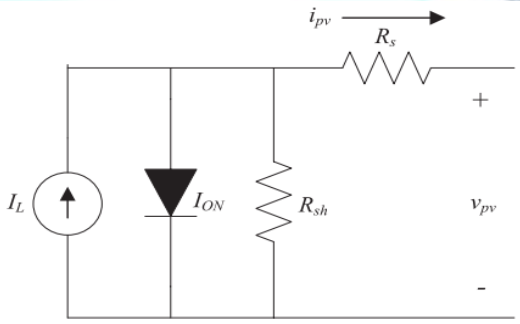

Fig. 2. Equivalent circuit diagram of the PV cell.

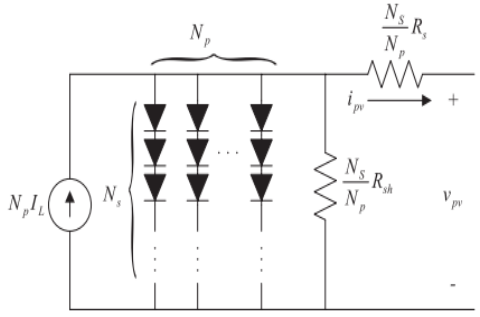

Fig. 3. Equivalent circuit diagram of the PV array.

by applying Kirchhoff's current law (KCL) in Fig. 2, the output current (*i*pv) generated by a PV cell can be written as

$$i_{\rm pv} = I_L - I_s\left[\exp\left[\alpha\left(v_{\rm pv} + R_s i_{\rm pv}\right)\right] - 1\right] - \frac{v_{\rm pv} + R_s i_{\rm pv}}{R_{\rm sh}}. \quad (2)$$

The light generated current *IL* depends on the solar irradiation that can be related by the following equation:

$$I_L = \left[I_{sc} + k_i\left(T_C - T_{\rm ref}\right)\right]\frac{s}{1000} \quad (3)$$

where *I*sc is the short-circuit current, *s* is the solar irradiation, *ki* is the cell's short-circuit current coefficient, and *T*ref is the reference temperature of the cell. The cell's saturation current *I*s varies with the temperature according to the following equation [17]:

$$I_s = I_{\rm RS}\left[\frac{T_C}{T_{\rm ref}}\right]^3 \exp\left[\frac{qE_g}{Ak}\left(\frac{1}{T_{\rm ref}} - \frac{1}{T_C}\right)\right] \quad (4)$$

Where *Eg* is the band gap energy of the semiconductor used in the reference temperature and solar irradiation. Since the output voltage of a PV cell is very low, a number of PV cells are connected together in series in order to obtain higher voltages. Then, they are encapsulated with glass, plastic, and other transparent materials to protect them from harsh environments and are called a PV module. To obtain the required voltage and power, a number of modules are connected in parallel to form a PV array. Fig. 3 shows an electrical equivalent circuit diagram of a PV array, where *N*s is the number of cells in series, and *Np* is the number of modules in parallel. In this case, the array *i*pv can be written as

$$i_{\rm pv} = N_p I_L - N_p I_s\left[\exp\left[\alpha\left(\frac{v_{\rm pv}}{N_s} + \frac{R_s i_{\rm pv}}{N_p}\right)\right] - 1\right] - \frac{N_p}{R_{\rm sh}}\left(\frac{v_{\rm pv}}{N_s} + \frac{R_s i_{\rm pv}}{N_p}\right). \quad (5)$$

B. Three-Phase Grid-Connected Photovoltaic System Model In the state-space form, Fig. 1 can be represented through the following equations [17], [18]:

$$\dot{i}_a = -\frac{R}{L}i_a - \frac{1}{L}e_a + \frac{v_{\rm pv}}{3L}(2K_a - K_b - K_c)$$
$$\dot{i}_b = -\frac{R}{L}i_b - \frac{1}{L}e_b + \frac{v_{\rm pv}}{3L}(-K_a + 2K_b - K_c)$$
$$\dot{i}_c = -\frac{R}{L}i_c - \frac{1}{L}e_c + \frac{v_{\rm pv}}{3L}(-K_a - K_b + 2K_c) \quad (6)$$

where *Ka, Kb*, and *Kc* are the input switching signals. Now, by applying KCL at the node where the dc link is connected, we obtain

$$\dot{v}_{\rm pv} = \frac{1}{C}\left(i_{\rm pv} - i_{\rm dc}\right). \quad (7)$$

However, the input current of the inverter *i*dc can be written as [19]

$$i_{\rm dc} = i_a K_a + i_b K_b + i_c K_c \quad (8)$$

which yields

$$\dot{v}_{\rm pv} = \frac{1}{C}i_{\rm pv} - \frac{1}{C}\left(i_a K_a + i_b K_b + i_c K_c\right) \quad (9)$$

The complete model of a three-phase grid-connected PV system can be presented by (6) and (9), which are nonlinear and time variant and can be converted into a time invariant model by applying *dq* transformation using the angular frequency (*ω*) of the grid, rotating the reference frame synchronized with grid where the *d* component of the grid voltage *Ed* is zero [17]. By using *dq* transformation, (6) and (9) can be written as

$$\dot{I}_d = -\frac{R}{L}I_d + \omega I_q - \frac{E_d}{L} + \frac{v_{\rm pv}}{L}K_d$$
$$\dot{I}_q = -\omega I_d - \frac{R}{L}I_q - \frac{E_q}{L} + \frac{v_{\rm pv}}{L}K_q$$
$$\dot{v}_{\rm pv} = \frac{1}{C}i_{\rm pv} - \frac{1}{C}I_d K_d - \frac{1}{C}I_q K_q \quad (10)$$

where *Idq* = *Tabc dq iabc, edq* = *Tabc dq eabc, Kdq* = *Tabc dq Kabc*. Equation (10) represents the complete mathematical model of a three-phase grid-connected PV system and this model is a nonlinear model due to the nonlinear behavior of the switching signals and the output current (*i*pv) of the PV array. The transformation matrix *T dqabc*

can be written as

$$T_{abc}^{dq} = \frac{2}{3}\begin{pmatrix} \cos\omega t & \cos(\omega t - 120) & \cos(\omega t + 120) \\ \sin\omega t & \sin(\omega t - 120) & \sin(\omega t + 120) \\ \frac{1}{2} & \frac{1}{2} & \frac{1}{2} \end{pmatrix} \quad (11)$$

At this point of mathematical modeling, the key issue the selection of the current component that can be obtained from the power delivered into the grid. Since *Ed* = 0, the real power delivered to the grid can be written as

$$P = \frac{3}{2} E_q I_q . \quad (12)$$

From (12), it can be seen that the maximum power delivery into the grid can be maintained by controlling the *q* component of the grid current, i.e., *Iq* . Based on this mathematical model, the overview of the partial feedback linearizing stabilization scheme is shown in the following section.

III. Overview of Partial Feedback Linearizing Stabilization Scheme

As the three-phase grid-connected PV system as represented by (10) has two control inputs (*Kd* and *Kq*) and two control outputs (*Iq* and *v*pv), the mathematical model can be represented by the following form of a nonlinear multi-input multi-output (MIMO) system

$$\begin{aligned} \dot{x} &= f(x) + g_1(x)u_1 + g_2(x)u_2 \\ y_1 &= h_1(x) \\ y_2 &= h_2(x) \end{aligned} \quad (13)$$

The partial feedback linearizing scheme transforms the nonlinear grid-connected PV system into a partially linearized PV system, and any linear controller design technique can be employed to obtain the linear control law for the partially linearized system. However, before obtaining a control law through partial feedback linearizing scheme, it is essential to ensure the partial feedback linearizability and internal dynamics stability of the PV system. The details of partial feedback linearizability and internal dynamics stability of the considered PV system are presented in [18] from where it can be seen that the PV system is partially linearized and that the internal dynamic of the PV systems is stable. The partially linearized PV system can be written

$$\begin{aligned} \dot{\tilde{z}}_1 &= -\omega I_d - \frac{R}{L} I_q - \frac{E_q}{L} + \frac{v_{pv}}{L} K_q = v_1 \\ \dot{\tilde{z}}_2 &= \frac{1}{C} i_{pv} - \frac{1}{C} I_d K_d - \frac{1}{C} I_q K_q = v_2 \end{aligned} \quad (14)$$

where $\tilde{z}$ represents the transformed states, and v represents the linear control inputs that are obtained through the PI design approach [18]. The nonlinear control law can be written as

$$\begin{aligned} K_d &= \frac{L}{v_{pv}}\left(v_1 + \omega I_d + \frac{R}{L} I_q + \frac{E_q}{L}\right) \\ K_q &= -\frac{C}{I_q}\left[v_2 + \frac{i_{pv}}{C} - \frac{L I_d}{C v_{pv}}\left(v_1 + \omega I_d + \frac{R}{L} I_q + \frac{E_q}{L}\right)\right]. \end{aligned} \quad (15)$$

Equation (15) is the final control law that is obtained through a partial feedback linearizing scheme, and the controller ensures the stability of the PV system for the considered nominal model and exact parameters of the system need to be known. However, in practice, it is very difficult to determine the exact parameters of the system. Thus, the considered partial feedback linearizing scheme is unable to maintain the stability of the PV system with changes in system conditions and the consideration of uncertainties within the PV system is necessary, which is shown in the following section.

IV. Uncertainty Modeling

In a practical PV system, atmospheric conditions change continuously for which there exists a variation in cell working temperature, as well as in solar irradiance. Because of changes in atmospheric conditions, the output voltage, current, and power of the PV unit changes significantly. For example, if a single module of a series string is partially shaded, and then its output current will be reduced, which will change the operating point of the whole string. Since the amount of the PV generation depends on solar irradiation that is uncertain, there are uncertainties in *i*pv which in turn causes uncertainties in the current (in the *dq*-frame, *Id* and *Iq*) injected into the grid. Moreover, as the values of the parameters used in the PV model are not exactly known, there are also parametric uncertainties. The PV system model as shown by (10) cannot capture these uncertainties. Therefore, it is essential to consider these uncertainties within the PV system model. In the presence of uncertainties, the nonlinear mathematical model of the three-phase grid-connected PV system, as

shown in (13), can be represented by the following equation:

$$\dot{x} = [f(x) + \Delta f(x)] + [g_1(x) + \Delta g_1(x)]u_1 + [g_2(x) + \Delta g_2(x)]u_2$$
$$y_1 = h_1(x)$$
$$y_2 = h_2(x) \quad (16)$$

$$\Delta g(x) = \begin{bmatrix} \Delta g_{11}(x) & 0 \\ 0 & \Delta g_{22}(x) \\ \Delta g_{31}(x) & \Delta g_{32}(x) \end{bmatrix}$$

The uncertainties need to be modeled in such a way that the controller will robustly stabilize the original system despite the uncertainties $\Delta f(x)$ and $\Delta g(x)$, i.e., the robust controller will attenuate the influence of system uncertainties. In order to achieve the control objective of robust stabilization, the structure of uncertainties and the locations of unknown parameters should satisfy the following conditions:

$$\Delta f(x) \quad \text{and} \quad \Delta g(x) \in \quad \text{span}\{g(x)\} \quad (17)$$

which is known as the matching condition [24]. If this matching condition holds, the following condition is true:

$$w \geq r = \rho \quad (18)$$

where r is the total relative degree of the nominal system, which is 2 [18], w is the relative degree of uncertainty $\Delta g(x)$, and ρ is the relative degree of uncertainty $\Delta f(x)$. In order to match the uncertainties with the PV system model, the relative degree of the uncertainty Δf should be 2 as it needs to equal to the relative degree of the nominal system in (10), which is 2. The relative degree of the uncertainty Δf can be calculated from the following equation:

$$L_{\Delta f} L_f^{1-1} h_1(x) = \Delta f_1$$
$$L_{\Delta f} L_f^{1-1} h_2(x) = \Delta f_3. \quad (19)$$

If the relative degree of Δf corresponding to the outputs $h1$ and $h2$ is 1, then the total relative degree of Δf will be 2, which will happen if $\Delta f1$ and $\Delta f3$ are not equal to zero. To match the uncertainty Δg, the relative degree of Δg should be equal to or greater than the relative degree of the nominal system and will be 2 if the following conditions hold:

$$L_{\Delta g} L_f^{1-1} h_1(x) = \Delta g_{11} \neq 0$$
$$L_{\Delta g} L_f^{1-1} h_2(x) = \Delta g_{31} + \Delta g_{32} \neq 0 \quad (20)$$

Where $\Delta g11$ must not be zero and either $\Delta g31$ or $\Delta g32$ can be zero, to match the uncertainty with the structure of the PV system. Since the proposed uncertainty modeling scheme considers the upper bound of the uncertainties, it is important to set these bounds, and the controller needs to be designed based on these bounds. If the maximum allowable changes in the system parameters is 30% and the variations in solar irradiation and environmental temperature are considered up to 80% of their nominal values. The partial feedback linearizing scheme as presented in [18] cannot stabilize the PV system appropriate if the aforementioned uncertainties are considered within the PV system model as the controller is designed to stabilize only the nominal system. However, in the robust partial feedback linearizing scheme, the aforementioned uncertainties need to be included to achieve the robust stabilization of the grid-connected PV system. The robust controller design by considering the aforementioned uncertainties within the grid-connected PV system model is shown in the following section.

V. Robust Controller Design

This section aims the derivation of the robust control law that robustly stabilizes a grid-connected PV system with uncertainties whose structures are already discussed in the previous section. The following steps are followed to design the robust controller for a three-phase grid-connected PV system.

1) *Step 1 (Partial feedback linearization of grid connected PV systems):* In this case, the partial feedback linearization for the system with uncertainties, as shown by (16), can be obtained as

$$\dot{\tilde{z}}_1 = L_f h_1(x) + L_{\Delta f} h_1(x) + [L_{g_1} h_1(x) + L_{\Delta g_1} h_1(x)]u_1 + [L_{g_2} h_1(x) + L_{\Delta g_2} h_1(x)]u_2$$
$$\dot{\tilde{z}}_2 = L_f h_2(x) + L_{\Delta f} h_2(x) + [L_{g_1} h_2(x) + L_{\Delta g_1} h_2(x)]u_1 + [L_{g_2} h_2(x) + L_{\Delta g_2} h_1(x)]u_2.$$

For the PV system, the partially linearized system can written as

$$\dot{\tilde{z}}_1 = -1.36\omega I_d - 1.042\frac{R}{L}I_q - 1.23\frac{E_q}{L} + 1.18\frac{v_{pv}}{L}K_q$$

$$\dot{\tilde{z}}_2 = \frac{1.16}{C}i_{pv} - \frac{1.08}{C}I_d K_d - \frac{1.14}{C}I_q K_q \quad (21)$$

If $v1$ and $v2$ are linear control inputs for the aforementioned partially feedback linearized system, (21) can be written as

$$v_1 = -1.36\omega I_d - 1.042\frac{R}{L}I_q - 1.23\frac{E_q}{L} + 1.18\frac{v_{pv}}{L}K_q$$

$$v_2 = \frac{1.16}{C}i_{pv} - \frac{1.08}{C}I_d K_d - \frac{1.14}{C}I_q K_q \quad (22)$$

Which can be obtained using any linear control technique, and in this paper, two PI controllers are used. However,

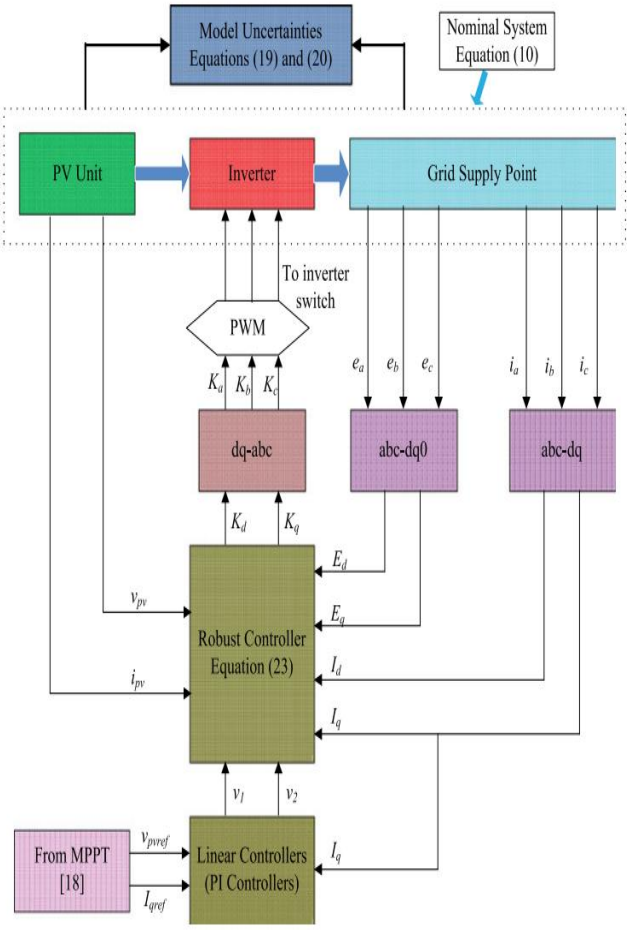

Fig. 4. Implementation block diagram.

before designing and implementing the controller based on partial feedback linearizing scheme, it is essential to check the stability of the internal dynamics that is similar to that described in [18].

2) *Step 2 (Derivation of robust control law):* From (22), the robust control law can be obtained as follows:

$$K_d = 0.85\frac{L}{v_{pv}}\left(v_1 + 1.36\omega I_d + 1.042\frac{R}{L}I_q + 1.23\frac{E_q}{L}\right)$$

$$K_q = -0.88\frac{C}{I_q}\left[v_2 + 1.16\frac{i_{pv}}{C} - 1.08\frac{I_d}{C}K_d\right] \quad (23)$$

Equation (23) is the final robust control law for a three grid connected PV system, and the control law contains the modeled uncertainties. The main difference between the designed robust control law (23) and the control law (15) is the inclusion of uncertainties within the PV system model. The performance of the designed robust stabilization scheme is evaluated and compared in the following section with our previously published partial feedback linearizing scheme with no uncertainties [18]. The performance of the controller is evaluated in the following section.

VI. Induction Motor

An induction motor is an example of asynchronous AC machine, which consists of a stator and a rotor. This motor is widely used because of its strong features and reasonable cost. A sinusoidal voltage is applied to the stator, in the induction motor, which results in an induced electromagnetic field. A current in the rotor is induced due to this field, which creates another field that tries to align with the stator field, causing the rotor to spin. A slip is created between these fields, when a load is applied to the motor. Compared to the synchronous speed, the rotor speed decreases, at higher slip values. The frequency of the stator voltage controls the synchronous speed. The frequency of the voltage is applied to the stator through power electronic devices, which allows the control of the speed of the motor. The research is using techniques, which implement a constant voltage to frequency ratio. Finally, the torque begins to fall when the motor reaches the synchronous speed. Thus, induction motor synchronous speed is defined by following equation,

$$n_s = \frac{120f}{P} \quad (24)$$

Where f is the frequency of AC supply, n, is the speed of rotor; p is the number of poles per phase of the motor. By varying the frequency of control circuit through AC supply, the rotor speed will change.

A. Control Strategy of Induction Motor

Power electronics interface such as three-phase SPWM inverter using constant closed loop Volts l

Hertz control scheme is used to control the motor. According to the desired output speed, the amplitude and frequency of the reference (sinusoidal) signals will change. In order to maintain constant magnetic flux in the motor, the ratio of the voltage amplitude to voltage frequency will be kept constant. Hence a closed loop Proportional Integral (PI) controller is implemented to regulate the motor speed to the desired set point. The closed loop speed control is characterized by the measurement of the actual motor speed, which is compared to the reference speed while the error signal is generated. The magnitude and polarity of the error signal correspond to the difference between the actual and required speed. The PI controller generates the corrected motor stator frequency to compensate for the error, based on the speed error.

VII. Simulation Results

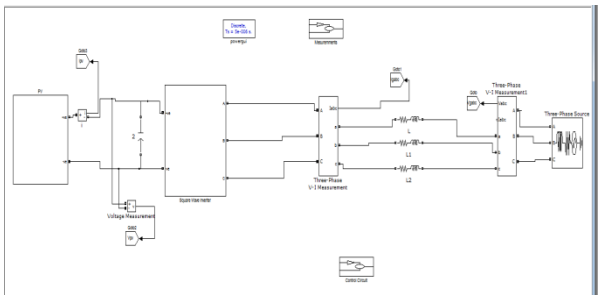

Fig 5 Matlab/simulation circuit of Adaptive Control Scheme for Pv Based system

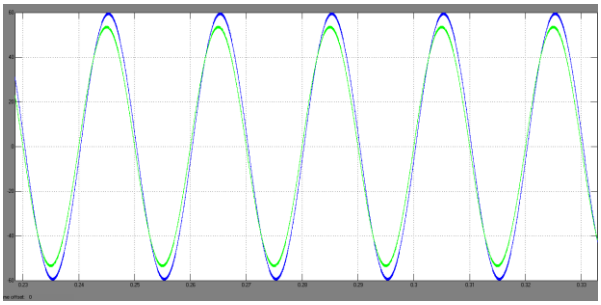

Fig 6 Performance under standard atmospheric conditions (Blue line—grid voltage, red line—grid current with the RPFBLSS, and green line—grid current with the PFBLS)

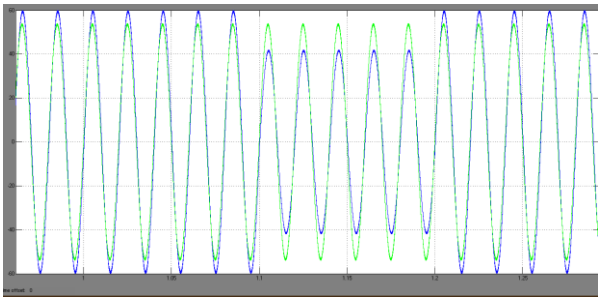

Fig 7 Performance under changing atmospheric conditions (Blue line—grid voltage, red line-grid current with the RPFBLSS, and green line—grid current with the PFBLS).

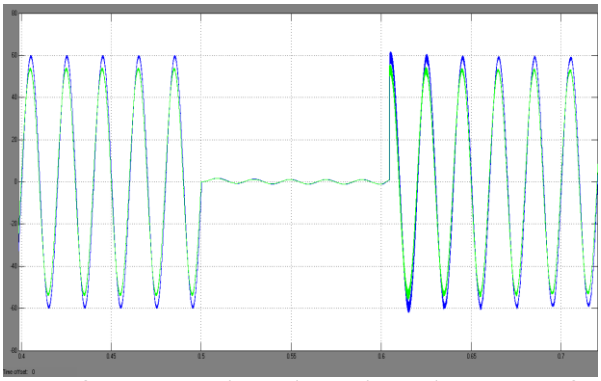

Fig 8 Performance under a three-phase short-circuit fault (Red line—grid current with the RPFBLSS, and green line—grid current with the PFBLS).

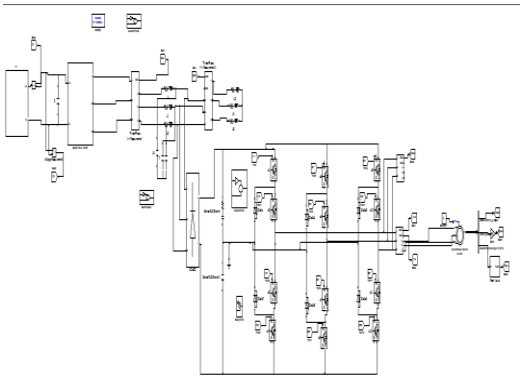

Fig 9 Matlab/simulation circuit of Adaptive Control Scheme for Pv Based system with Induction Motor

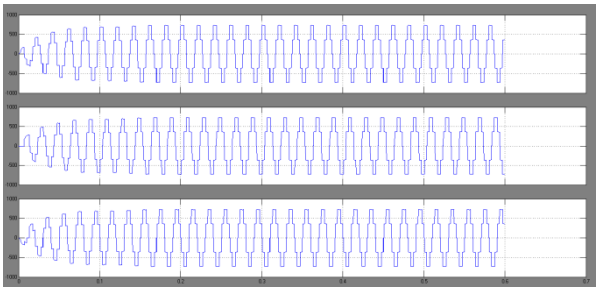

Fig 10 simulation wave form of line output voltage with IM

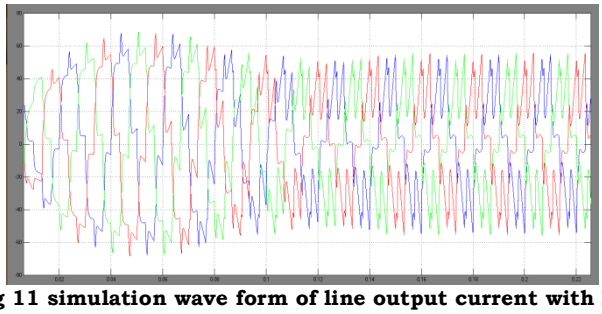

Fig 11 simulation wave form of line output current with IM

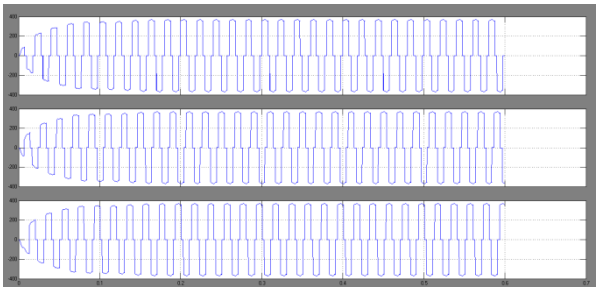

Fig 12 simulation wave form of phase voltage with IM

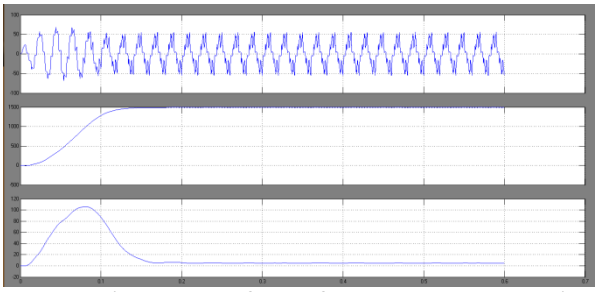

Fig 13 simulation wave form of stator current, speed and torque

VIII. CONCLUSION

In this paper, a robust stabilization scheme is considered by modeling the uncertainties of a three phase grid-connected PV system based on the satisfaction of matching conditions to ensure the operation of the system at unity power factor. In order to design the robust scheme, the partial feedback linearization approach is used, and with the designed scheme, only the upper bounds of the PV systems' parameters and states need to be known rather than network parameters, system operating points, or nature of the faults. The resulting robust scheme enhances the overall stability of a three-phase grid connected PV system, considering admissible network uncertainties. Thus, this stabilization scheme has good robustness against the PV system parameter variations, irrespective of the network parameters and configuration. Future work will include the implementation of the proposed scheme on a Induction machine system to study the characteristics of speed, torque.

REFERENCES

[1] S. Jain and V. Agarwal, "A single-stage grid connected inverter topology for solar PV systems with maximum power point tracking," *IEEE Trans. Power Electron.*, vol. 22, no. 5, pp. 1928–1940, Sep. 2007.

[2] S. B. Kjaer, J. K. Pedersen, and F. Blaabjerg, "A review of single-phase grid-connected inverters for photovoltaic modules," *IEEE Trans. Ind. Appl.*, vol. 41, no. 5, pp. 1292–1306, Sep./Oct. 2005.

[3] T. Esram and P. L. Chapman, "Comparison of photovoltaic array maximum power point tracking techniques," *IEEE Trans. Energy Convers.*, vol. 22, no. 2, pp. 439–449, Jun. 2007.

[4] I. Houssamo, F. Locment, and M. Sechilariu, "Maximum power point tracking for photovoltaic power system: Development and experimental comparison of two algorithms," *Renewable Energy*, vol. 35, no. 10, pp. 2381–2387, Oct. 2010.

[5] U. Zimmermann and M. Edoff, "A maximum power point tracker for long-term logging of PV module performance," *IEEE J. Photovoltaics*, vol. 2, no. 1, pp. 47–55, Jan. 2012.

[6] E. Koutroulis and F. Blaabjerg, "A new technique for tracking the global maximum power point of PV arrays operating under partial-shading conditions," *IEEE J. Photovoltaics*, vol. 2, no. 2, pp. 184 190, Apr. 2012.

[7] L. F. L. Villa, D. Picault, B. Raison, S. Bacha, and A. Labonne, "Maximizing the power output of partially shaded photovoltaic plants through optimization of the interconnections among its modules," *IEEE J. Photovoltaics*, vol. 2, no. 2, pp. 154–163, Apr. 2012.

[8] F. Blaabjerg, R. Teodorescu, M. Liserre, and A. V. Timbus, "Overview of control and grid synchronization for distributed power generation systems," *IEEE Trans. Ind. Electron.*, vol. 53, no. 5, pp. 1398–1409, Oct. 2006.

[9] A. Kotsopoulos, J. L. Darte, and M. A. M. Hendrix, "Predictive DC voltage control of single-phase PV inverters with small dc link capacitance," in *Proc. IEEE Int. Symp. Ind. Electron.*, Jun. 2003, pp. 793–797.

[10] C. Meza, J. J. Negroni, D. Biel, and F. Guinjoan, "Energy balance modeling and discrete control for single-phase grid connected PV central inverters," *IEEE Trans. Ind. Electron.*, vol. 55, no. 7, pp. 2734–2743, Jul. 2008.

[11] R. Kadri, J. P. Gaubert, and G. Champenois, "An improved maximum power point tracking for photovoltaic grid-connected inverter based on voltage-oriented control," *IEEE Trans. Ind. Electron.*, vol. 58, no. 1, pp. 66–75, Jan. 2011.

[12] J. Selvaraj and N. A. Rahim, "Multilevel inverter for grid-connected PV system employing digital PI controller," *IEEE Trans. Ind. Electron.*, vol. 56, no. 1, pp. 149–158, Jan. 2009.

[13] N. A. Rahim, J. Selvaraj, and C. C. Krismadinata, "Hysteresis current control and sensorless MPPT for grid-connected photovoltaic systems," in *Proc. IEEE Int. Symp. Ind. Electron.*, 2007, pp. 572–577.

[14] A. Kotsopoulos, J. L. Duarte, and M. A. M. Hendrix, "A predictive control scheme for DC voltage and AC current in grid-connected photovoltaic inverters with minimum DC link capacitance," in *Proc. IEEE Ind. 27th Annu. Conf. Electron. Soc.*, 2001, pp. 1994–1999.

[15] I. Kim, "Sliding mode controller for the single-phase grid connected photovoltaic system," *Appl. Energy*, vol. 83, pp. 1101 1115, 2006.

[16] A. O. Zue and A. Chandra, "State feedback linearization control of a grid connected photovoltaic interface with MPPT," in *Proc. IEEE Electr. Power Energy Conf.*, Oct. 2009.

[17] D. Lalili, A. Mellit, N. Lourci, B. Medjahed, and E. M. Berkouk, "Input output feedback linearization control and variable step size MPPT algorithm of a grid-connected photovoltaic inverter," *Renewable Energy*, vol. 36, no. 12, pp. 3282–3291, Dec. 2011.

[18] M. A. Mahmud, H. R. Pota, and M. J. Hossain, "Dynamic stability of three-phase grid-connected photovoltaic system using zero dynamic design

approach," *IEEE J. Photovoltaics*, vol. 2, no. 4, pp. 564–571, Oct. 2012.

[19] I.-S. Kim, "Robust maximum power point tracker using sliding mode controller for the three–phase grid–connected photovoltaic system," *Sol. Energy*, vol. 81, no. 3, pp. 405–414, Mar. 2007.

[20] C.-C. Chu and C.-L. Chen, "Robust maximum power point tracking method for photovoltaic cells: A sliding mode control approach," *Sol. Energy*, vol. 83, no. 8, pp. 1370–1378, Aug. 2009.

[21] M. J. Hossain, T. K. Saha, N. Mithulananthan, and H. R. Pota, "Robust control strategy for PV system integration in distribution systems," *Appl. Energy*, vol. 99, pp. 355–362, Nov. 2012.

[22] A. Yazdani and P. P. Dash, "A control methodology and characterization of dynamics for a photovoltaic (PV) system interfaced with a distribution network," *IEEE Trans. Power Del.*, vol. 24, no. 3, pp. 1538–1551, Jul. 2009.

[23] Y.-K. Chen, C.-H. Yang, and Y.-C. Wu, "Robust fuzzy controlled photovoltaic power inverter with Taguchi method," *IEEE Trans. Aerosp. Electron. Syst.*, vol. 38, no. 3, pp. 940–954, Jul. 2002. [24] S. Behtash, "Robust output tracking for nonlinear systems," *Int. J. Control*, vol. 51, no. 6, pp. 1381–1407, 1990.